Preprints of the 21st IFAC World Congress (Virtual)
Berlin, Germany, July 12-17, 2020

Model Predictive Trajectory Tracking for a Ground Vehicle in a Heterogeneous Rendezvous with a Fixed-Wing Aircraft ⋆

Christoph Hebisch * **Dirk Abel** *

* *Institute of Automatic Control, RWTH Aachen University, Aachen, Germany (e-mail: {c.hebisch, d.abel}@irt.rwth-aachen.de)*

Abstract: The maneuver of landing a fixed-wing unmanned aerial vehicle (UAV) autonomously on a moving ground platform requires precise spatial synchronization of both agents. Depending on the desired control strategy for the maneuver, the unmanned ground vehicle (UGV) must be capable to track the UAV's trajectory robustly with respect to the ground plane even in the presence of disturbances such as wind gusts. In this paper, a linear model predictive trajectory tracking controller for a UGV based on a kinematic bicycle model is presented, assuming that the UAV aims at following a straight flight path with a given velocity. The vehicle model is discretized and linearized in each sampling step, resulting in a quadratic optimization problem which yields the optimal steering angle and motor current demand of the UGV. In the optimization problem, actuator constraints as well as hardware-related dead-times are taken into account. By constraining the yaw rate of the UGV, sideslip of the UGV is prevented, preserving the consistency of the kinematic model. Main requirements for the controller are the ability to allow sufficiently precise trajectory tracking with a longitudinal and lateral deviation of less than 0.5 m, i.e., within the dimensions of the landing platform in the given hardware setup, and real-time capability. Hardware-in-the-loop simulations and experimental results with a model-scale ground vehicle are presented that indicate the validity of the proposed control scheme.

Keywords: Automotive Control, Autonomous Vehicles, Model-Based Control, Predictive Control, Trajectory Tracking and Path Following

1. INTRODUCTION

Development efforts towards enabling the automated landing of a fixed-wing aircraft on a moving ground platform are strongly driven by the advantages which a substantial reduction or complete omission of the landing gear would imply, i.e., an increase in payload or flight duration. The landing maneuver of a synchronized aircraft on a ground vehicle is called heterogeneous rendezvous. Especially in the case of High Altitude Long Endurance (HALE) missions, the mass of the landing gear can pose a significant share of the take-off mass compared to the payload (Muskardin et al. (2017)) and is therefore a major drawback. The reduction of the undercarriage has the potential to improve fuel efficiency in air traffic by reducing aircraft mass and allowing a smaller dimensioning of the propulsion systems as a consequence. Furthermore, the use of a ground-based landing gear could improve safety in crosswind landing scenarios.

Recent research regarding the heterogeneous rendezvous problem includes a cross-coupled PID control strategy for synchronizing the vehicles (Muskardin et al. (2017)), where the ground vehicle is operated by a human driver who manually controls the steering wheel, throttle, and brake based on commands displayed on a screen mounted in the car.

Fig. 1. The model-scale experimental UGV *IRT-Buggy* equipped with a landing platform measuring 1m × 1m

An MPC based approach was presented by Persson et al. (2017) that showed simulative results indicating the feasibility and benefits of a model predictive control strategy, i.e., the inclusion of optimality requirements and constraints as well as explicit task allocation to the vehicles, but lacks real-time capability. An approach towards full automation of the ground vehicle considering real-time capability utilizes a PID controller to track an optimized reference trajectory (Persson and Wahlberg (2018)).

Reiter et al. (2016a) have proposed an experimental setup for the initiation of a heterogeneous rendezvous with a model-scale ground vehicle (Reiter et al. (2014)), depicted in Fig. 1, and aircraft, where the lateral positions of

⋆ This work is supported by the German Research Foundation (DFG), project number 391925917.

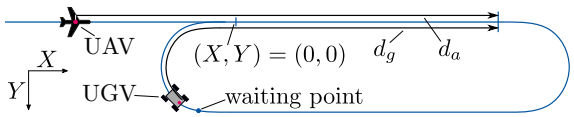

Fig. 2. Schematic overview of the rendezvous initiation setup by Reiter et al. (2016a)

both vehicles are controlled indepedently, emulating the functionality of magnetic levitation (MAGLEV) based systems for assisted take-off and landing of fixed-wing aircrafts (Rohacs et al. (2014)). Fig. 2 shows an overview of the rendezvous initiation setup. This setup provides a flexible hardware and software framework for further experiments and is therefore used in this work to control the vehicles to an operating point from which the actual trajectory tracking controller can take over since the MPC requires sufficient proximity of the vehicles due to the linearization of the prediction models (see Section 2).

A comparison between linear and non-linear model predictive path tracking controllers by Falcone et al. (2006) based on a dynamic bicycle model indicated similar performance for the linear and non-linear approach for a prediction horizon of 2.5 s, which is comparable to the one used in this work (see Section 3.1), but mainly considered higher velocities and slippery road conditions. Regarding the advantages and disadvantages of kinematic and dynamic bicycle models in the context of model predictive control for autonomous ground vehicles, Kong et al. (2015) conclude that a kinematic model can yield accurate state predictions if the lateral acceleration of the vehicle remains sufficently low. For too large lateral accelerations, sideslip is induced, making the ground vehicle's motion non-kinematic, which must be considered at the required velocity during the heterogeneous rendezvous. In order to preserve the consistency of the kinematic bicycle model, Polack et al. (2017) propose a heuristical upper limit on the lateral acceleration depending on the road friction.

Based on the rendezvous initiation setup by Reiter et al. (2016a), where the UAV tries to follow a predefined track closely (see Fig. 2) with a given velocity, the trajectory tracking controller for the UGV must be able to compensate longitudinal and lateral deviations as well as deviations in terms of velocity and heading between the vehicles. These deviations are mainly caused by disturbances such as wind gusts.

In this work, we investigate the feasibility of a linear model predictive controller for a UGV in a heterogeneous rendezvous. Principal requirements for the controller are the ability to allow sufficiently precise trajectory tracking with a longitudinal and lateral deviation of less than 0.5 m, i.e., within the dimensions of the landing platform in the given hardware setup (see Fig. 3), and real-time capability. In order to fulfill real-time requirements, we propose the use of a kinematic bicycle model for the UGV. By constraining the lateral acceleration of the UGV in the optimization problem of the MPC, the consistency of the kinematic model is maintained.

As described by Persson et al. (2017), optimization based control strategies for the solution of the heterogeneous rendezvous problem entail the advantage that the control effort and the synchronization task (for each degree

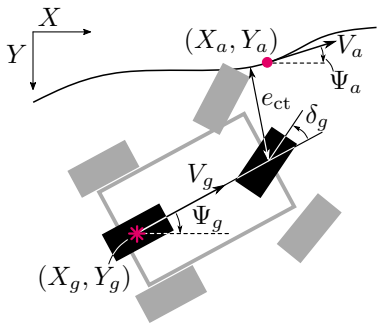

Fig. 3. The kinematic bicycle model and vehicle states in a local cartesian coordinate system

of freedom) can explicitly be allocated through the cost function, which furthermore allows adaption in case of actuator failures or disturbances. Especially in the presence of disturbances such as wind gusts, the UAV might not be capable to actively take part in the control effort. Thus, the ground vehicle is required to precisely follow the trajectory of the UAV. For this purpose, hardware-in-the-loop (HiL) simulations as well as real-world experiments are presented with an experimental vehicle platform (Fig.1), proving the applicability of the proposed control strategy in terms of tracking performance and real-time capability.

2. UNMANNED GROUND AND AERIAL VEHICLE MODEL

According to the kinematic bicycle model with the center of the rear axis as the reference point, depicted in Fig. 3, the UGV's dynamics are modeled by the following time-continuous equations:

$$\dot{X}_g = V_g \cos(\Psi_g) \tag{1a}$$
$$\dot{Y}_g = V_g \sin(\Psi_g) \tag{1b}$$
$$\dot{V}_g = f(V_g, I_g^{\mathrm{des}}) \tag{1c}$$
$$\dot{\Psi}_g = \frac{V_g}{L} \tan(\delta_g) \tag{1d}$$
$$\dot{\delta}_g = \frac{1}{T_\delta}(\delta_g^{\mathrm{des}} - \delta_g), \tag{1e}$$

where X_g and Y_g denote the vehicle's longitudinal and lateral position in local cartesian coordinates, respectively, V_g denotes the velocity, Ψ_g the yaw angle, and δ_g the steering angle. Subscripts g and a denote variables regarding the ground and aerial vehicle, respectively. The distance between the front and rear axis of the ground vehicle is $L = 0.73$ m. The steering dynamics can be approximated by a first-order system with the desired steering angle δ_g^{des} as the input and time constant $T_\delta = 0.1$ s and the propulsion dynamics are described by the linear function f which has the velocity v_g and the desired motor current I_g^{des} as inputs (Reiter et al. (2016a)). For real-world experiments, the center of the landing platform can be computed straightforwardly by projecting the reference point (X_g,Y_g), which coincides with the position of the GNSS antenna, along the UGV's longitudinal axis.

Based on the observed current state (X_a, Y_a, V_a, Ψ_a) of the UAV, a simple prediction model given by the equations

$$\dot{X}_a = V_a \cos(\Psi_a) \tag{2a}$$
$$\dot{Y}_a = V_a \sin(\Psi_a) \tag{2b}$$

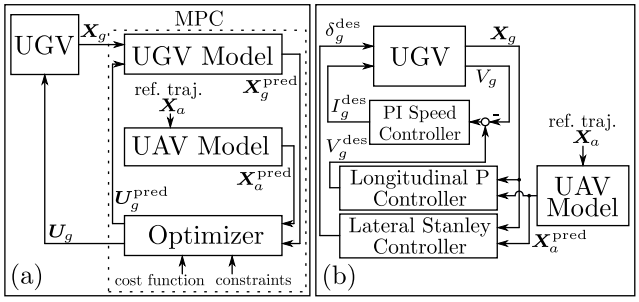

Fig. 4. Block diagrams of the presented MPC (a) and Stanley based trajectory tracking controller (b)

$$\dot{V}_a = A_a^{\text{const}} \tag{2c}$$
$$\dot{\Psi}_a = \dot{\Psi}_a^{\text{const}} \tag{2d}$$

is used to predict the UAVs motion as a reference for the trajectory tracking controller, assuming constant acceleration A_a^{const} and yaw rate $\dot{\Psi}_a^{\text{const}}$ in each prediction frame.

Combining the state vectors $\boldsymbol{X}_g = [X_g, Y_g, V_g, \Psi_g, \delta_g]^T$ and $\boldsymbol{X}_a = [X_a, Y_a, V_a, \Psi_a]^T$ of the ground and aerial vehicle, respectively, the joint state vector is defined as

$$\boldsymbol{X} = [X_g, Y_g, V_g, \Psi_g, \delta_g, X_a, Y_a, V_a, \Psi_a]^T \tag{3}$$

and the control input vector as

$$\boldsymbol{U} = \left[I_g^{\text{des}}, \delta_g^{\text{des}}\right]^T. \tag{4}$$

3. TRAJECTORY TRACKING CONTROL

In the following subsections, a model-predictive trajectory tracking controller as well as a controller based on the Stanley method (Hoffmann et al. (2007)) are presented, which are subsequently compared against each other by means of an experimentally recorded reference trajectory of the aircraft, which represents typical wind conditions. An overview of the controllers is depicted in Fig. 4.

3.1 Model Predictive Controller

Model predictive controllers are based on the concept of minimizing a cost function J over a receding prediction horizon, yielding the optimal control input $U^\star$ considering a given set of constraints. Generally, the cost function penalizes deviations of the control variable from a desired trajectory and changes of the control input. In order to predict future deviations of the control variable from the desired trajectory, the linear MPC relies on a linear discrete-time prediction model of the system to be controlled.

For the proposed linear MPC, we define

$$\boldsymbol{e} = \begin{bmatrix} X_a - X_g \\ Y_a - Y_g \\ V_a - V_g \\ \Psi_a - \Psi_g \end{bmatrix} = \begin{bmatrix} \Delta X \\ \Delta Y \\ \Delta V \\ \Delta \Psi \end{bmatrix} \tag{5}$$

as the synchronization error, that shall be driven to zero. Through linearization of the vehicle models defined in (1) and (2), we can straightforwardly formulate the state space representation

$$\dot{\boldsymbol{x}} = \mathbf{A}\boldsymbol{x} + \mathbf{B}\boldsymbol{u}, \quad \boldsymbol{x} = \boldsymbol{X} - \boldsymbol{X}_0 \tag{6}$$

around an operating point $\boldsymbol{X}_0$. The discrete-time state-space model is then given as

$$\boldsymbol{x}_{k+1} = \mathbf{A}_D \boldsymbol{x}_k + \mathbf{B}_D \boldsymbol{u}_k \tag{7}$$

with

$$\mathbf{A}_D = \mathrm{e}^{\mathbf{A}T_{\text{MPC}}}, \quad \mathbf{B}_D = (\mathrm{e}^{\mathbf{A}T_{\text{MPC}}} - \mathbf{I})\mathbf{A}^{-1}\mathbf{B}. \tag{8}$$

It is assumed that all states can be measured directly with sufficient accuracy, which is applicable with the given hardware. Since the experimental ground vehicle contains a hardware-related input dead-time of approximately $T_d = 0.055$ s, which can cause oscillating behavior of the closed loop system, additional states for control inputs from the previous prediction frame are added to the system. With a sample time of $T_{\text{MPC}} = 0.05$ s for the MPC, the control inputs of the previous time step are considered, yielding the modified state-space model

$$\tilde{\boldsymbol{x}}_{k+1} = \underbrace{\begin{bmatrix} \mathbf{A}_D & \mathbf{B}_D \\ \mathbf{0}^{2\times 9} & \mathbf{0}^{2\times 2} \end{bmatrix}}_{\tilde{\mathbf{A}}} \tilde{\boldsymbol{x}}_k + \underbrace{\begin{bmatrix} \mathbf{0}^{9\times 2} \\ \mathbf{I}^{2\times 2} \end{bmatrix}}_{\tilde{\mathbf{B}}} \boldsymbol{u}_k \tag{9}$$

with the modified state vector

$$\tilde{\boldsymbol{x}}_k = \begin{bmatrix} \boldsymbol{x}_k \\ \boldsymbol{u}_{k-1} \end{bmatrix}. \tag{10}$$

With the linear state-space model defined in (9)-(10), the quadratic optimization problem

$$\begin{aligned} \min_{U,\xi} \quad & J(\tilde{\boldsymbol{x}}, \boldsymbol{u}) = \sum_{i=H_1}^{H_2} \|\boldsymbol{e}_{k+i|k} - \boldsymbol{w}_{k+i|k}\|_{\mathbf{Q}}^2 \\ & + \sum_{i=0}^{H_u-1} \|\Delta \boldsymbol{u}_{k+i|k}\|_{\mathbf{R}}^2 + \xi^2 \\ \text{s.t.} \quad & \boldsymbol{U}^{\min} \le \boldsymbol{u}_{k+i|k} + \boldsymbol{U}_{k|k} \le \boldsymbol{U}^{\max} \\ & \frac{\left|\boldsymbol{u}_{(k+i+1)|k} - \boldsymbol{u}_{k+i|k}\right|}{T_{\text{MPC}}} \le \dot{\boldsymbol{U}}^{\max} \\ & \frac{\left|\Psi_{g,(k+i+1)|k} - \Psi_{g,k+i|k}\right|}{T_{\text{MPC}}} \le \dot{\Psi}_g^{\max} + \xi, \ \xi \ge 0 \end{aligned} \tag{11}$$

with $\Delta \boldsymbol{u}_{k+i|k} = \boldsymbol{u}_{k+i|k} - \boldsymbol{u}_{k+i-1|k}$ and slack variable ξ is formulated for each time step k by successive online linearization of the vehicle models , and subsequently solved. The control input constraints are defined as

$$\boldsymbol{U}^{\min} = \left[I_g^{\min}, \delta_g^{\min}\right]^T \tag{12a}$$
$$\boldsymbol{U}^{\max} = \left[I_g^{\max}, \delta_g^{\max}\right]^T \tag{12b}$$
$$\dot{\boldsymbol{U}}^{\max} = \left[\dot{I}_g^{\max}, \dot{\delta}_g^{\max}\right]^T \tag{12c}$$

and ensure the technical feasibility of the controller and smooth steering by limiting steering angle and rate. In order to prevent side slip and preserve the consistency of the kinematic bicycle model, according to a heuristic proposed by Polack et al. (2017) the lateral acceleration a_g^{lat} of the ground vehicle should be kept below 0.5μg, where μ is the road friction coefficient and g the gravitational acceleration. Since the lateral acceleration of the ground vehicle is not explicitly predicted by the given model, the yaw rate is conservatively constrained to

$$\dot{\Psi}_g^{\max} = \frac{0.5\mu \mathrm{g}}{V_g^{\max}} \approx 20 \frac{\mathrm{deg}}{\mathrm{s}}, \tag{13}$$

assuming $\mu = 0.7$ and a maximum velocity of $V_g^{\max,\text{RV}} = 10 \frac{\mathrm{m}}{\mathrm{s}}$ during the rendezvous maneuver. By employing a reference function

$$\boldsymbol{w}_{k+i|k} = \alpha^i \boldsymbol{e}_{k|k} \tag{14}$$

a smoother response of the system can be achieved by choosing a positive constant value for $\alpha < 1$, which corresponds to low-pass filtering of the reference (Camacho and Alba (2013)). The optimization problem yields the optimal control sequence

$$U^\star = \{\boldsymbol{u}^\star_{k|k}, \dots, \boldsymbol{u}^\star_{(k+N_u-1)|k}\} \tag{15}$$

from which only the first value is applied to the system. Based on the conducted simulations, the weighting matrices are chosen as

$$\mathbf{Q} = \mathrm{diag}(100000, 50000, 1, 1) \tag{16a}$$
$$\mathbf{R} = \mathrm{diag}(1, 100000) \tag{16b}$$

The remaining parameters of the MPC are summarized in Table 1.

3.2 Stanley Controller

The lateral Stanley controller (Hoffmann et al. (2007)) is an intuitive and computationally simple non-linear steering control law named after the DARPA Grand Challenge 2005 (Buehler et al. (2007)) winning autonomous vehicle from Stanford University. By feed-forwarding the heading error $\Delta\Psi$ between a reference trajectory and the ground vehicle, and a non-linear feed-back function

$$\delta_g^{\mathrm{fb}} = \arctan \frac{k_{\mathrm{lat}} e_{\mathrm{ct}}}{V_g} \tag{17}$$

of the cross-track error e_{ct} with respect to the center of the front axis and the current velocity V_g with gain parameter k_{lat}, the steering angle demand is computed as

$$\delta_g^{des} = \begin{cases} \Delta\Psi + \delta_g^{\mathrm{fb}} & \text{if} \quad \left|\Delta\Psi + \delta_g^{\mathrm{fb}}\right| < \delta_g^{\max} \\ \delta_g^{\max} & \text{if} \quad \Delta\Psi + \delta_g^{\mathrm{fb}} \geq \delta_g^{\max} \\ -\delta_g^{\max} & \text{if} \quad \Delta\Psi + \delta_g^{\mathrm{fb}} \leq -\delta_g^{\max}. \end{cases} \tag{18}$$

When the cross-track error increases, the controller demands a larger steering angle. However, an increase of the velocity decreases the feed-back term in order to reduce lateral forces. For the conducted experiments, the gain parameter was set to $k_{\mathrm{lat}} = 0.5$, as higher values of k_{lat} caused oscillating steering behavior in the conducted experiments due to the dead-time in the system. Nevertheless, it should be kept in mind that the choice of k_{lat} does not guarantee similar behavior in other scenarios (Snider et al. (2009)).

For longitudinal synchronization, a P controller with the velocity v_a of the aerial vehicle as feed-forward is used (Reiter et al. (2016a); Muskardin et al. (2017)), yielding

$$V_g^{\mathrm{des}} = V_a + k_{\mathrm{lon}} \cdot \Delta X \cdot \mathrm{s}^{-1} \tag{19}$$

Table 1. MPC parameters

Parameter	Symbol	Value
MPC sample time	T_{MPC}	0.05 s
lower prediction horizon	H_1	3
upper prediction horizon	H_2	20
control horizon	H_c	5
max. yaw rate	$\dot{\Psi}_g^{\max}$	20 $\frac{\mathrm{deg}}{\mathrm{s}}$
min./max. steering angle	$\delta_g^{\min}/\delta_g^{\max}$	± 10 deg
max. steering rate	$\dot{\delta}_g^{\max}$	10 $\frac{\mathrm{deg}}{\mathrm{s}}$
min./max. motor current	$I_g^{\min}/I_g^{\max}$	± 60 A
max. motor current change rate	$\dot{I}_g^{\max}$	60 $\frac{\mathrm{A}}{\mathrm{s}}$
reference function parameter	α	0.5

with unity gain $k_{\mathrm{lon}} = 1$. The velocity demand v_g^{des} is adjusted by a PI speed controller implemented on the low-level control of the vehicle. As the trajectory of the UAV is only known up to the current time, the model given in (2) is used to predict the trajectory of the UAV when the UGV is ahead in longitudinal direction.

4. PRACTICAL IMPLEMENTATION

For validation of the proposed model-predictive trajectory tracking controller, hardware-in-the-loop simulations (Reiter et al. (2016b)) as well as real-world experiments using the experimental vehicle *IRT-Buggy* (1) were conducted. The vehicle has a total length of approximately 1.0 m, a width of 0.8 m, and weighs approximately 60 kg. Two brushless DC motors enable a maximum velocity of approximately $V_g^{\max} = 12 \frac{\mathrm{m}}{\mathrm{s}}$ and a maximum acceleration of $A_g^{\max} = 2 \frac{\mathrm{m}}{\mathrm{s}^2}$.

In the experimental setup, localization is provided by an RTK GPS receiver with centimeter level accuracy.

An experimentally recorded trajectory of a model-scale airplane corresponding to the setup described in Reiter et al. (2016a) with a runway length of approximately 90 m was taken as a reference. The control algorithms are implemented on an embedded PC equipped with an Intel Atom N450 dual-core processor clocked at 1.66 GHz running Simulink Real-Time with a main sample rate of 100 Hz. As for the solver for the optimization problem of the MPC, qpOASES (Ferreau et al. (2014)) was used within the scope of this work.

As the trajectory tracking controller assumes an operating point where the UAV and UGV are in close proximity, the rendezvous initiation controller proposed by Reiter et al. (2016a) is utilized. A schematic overview of the setup is depicted in Fig. 2. This setup allows the automated execution of multiple consecutive test runs as the ground vehicle automatically returns to the defined waiting point on the map. In order to prevent the trajectory tracking controller from being in saturation during the acceleration of the ground vehicle, the velocity demand for the ground vehicle is given as

$$V_g^{\mathrm{des}} = \begin{cases} V_a - \sqrt{2 \cdot A_g^{\mathrm{des}} \cdot \Delta d} & \text{if} \quad \Delta d > 0 \\ 0 & \text{otherwise,} \end{cases} \tag{20}$$

where $\Delta d = d_a - d_g$ is the map-based distance of the vehicles with respect to the end of the runway. A reasonable value $A_g^{\mathrm{des}} = 1 \frac{\mathrm{m}}{\mathrm{s}^2}$ for the acceleration demand during the initiation phase was used for the experiments. As soon as a sufficient proximity of the vehicles, defined as

$$\Delta X < 0.1 \text{ m} \tag{21a}$$
$$\Delta Y < 0.1 \text{ m} \tag{21b}$$
$$\Delta V < 0.2 \ \frac{\mathrm{m}}{\mathrm{s}} \tag{21c}$$
$$\Delta\Psi < 2 \text{ deg}, \tag{21d}$$

is reached, the actual trajectory tracking control law is applied for the remainder of the maneuver. Ideally, the proximity condition is met at the point $(X, Y) = (0, 0)$ shown in Fig. 2.

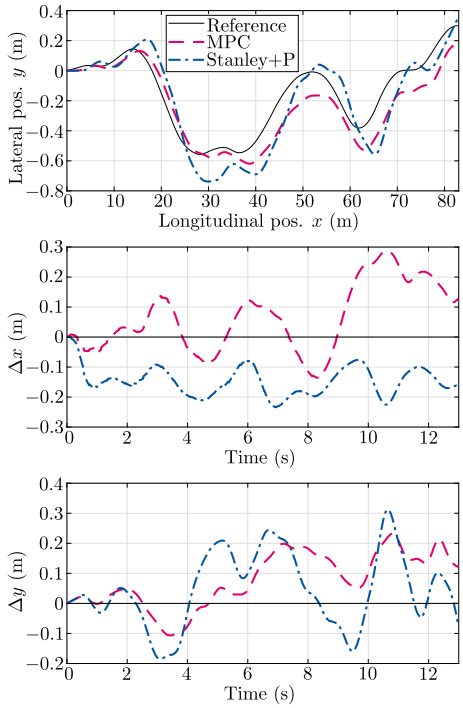

Fig. 5. Hardware-in-the-loop simulation results for the MPC and Stanley controller

5. RESULTS

5.1 Simulative Results

A comparison of the HiL simulation results in terms of longitudinal and lateral deviation from the reference trajectory for the MPC and the Stanley controller is depicted in Fig. 5. The root mean square and maximum absolute control errors ΔX, ΔY, ΔV, and $\Delta\Psi$ between the ground vehicle and the reference trajectory are given in Tables 2 and 3.

Results of the simulations indicate similar tracking performance for the model predictive controller and the Stanley based controller regarding RMS and maximum absolute error, with the MPC showing slightly better tracking with respect to the RMS longitudinal and lateral error. Based on the simulations, both controllers would allow sufficiently close trajectory tracking for landing the UAV on the ground vehicle throughout the complete reference trajectory, as the maximum absolute longitudinal and lateral error remain within the dimensions of the landing platform (see Fig. 1). The remaining control offset of the MPC in lateral direction can be ascribed to remaining model errors. However, it can be observed that the Stanley based controller shows more overshoot in case of directional changes in the reference trajectory caused by wind gusts. This occurs due to errors induced by the simple prediction model of the UAV when the UGV is longitudinally ahead of the UAV. Based on the promising simulative results, the MPC was considered for further real-world experiments.

Table 2. RMS and maximum absolute control error in HiL simulations with MPC

	ΔX(m)	ΔY(m)	$\Delta V(\frac{\text{m}}{\text{s}})$	$\Delta\Psi$(deg)
RMS	0.130	0.120	0.151	2.387
|max|	0.286	0.233	0.382	5.327

Table 3. RMS and maximum absolute control error in HiL simulations with Stanley based controller

	ΔX(m)	ΔY(m)	$\Delta V(\frac{\text{m}}{\text{s}})$	$\Delta\Psi$(deg)
RMS	0.155	0.131	0.134	2.775
|max|	0.235	0.313	0.491	6.467

5.2 Experimental Results

Experimental results for the model-predictive trajectory tracking controller are depicted in Fig. 6 and the RMS and maximum absolute control errors are summarized in Table 4. For the optimization problem, the same parameters were used as in the simulations.

The initial offset between the UGV and the reference trajectory in the experimental setup is caused by the conditions defined in (21) for the switching between the initiation controller and the actual trajectory tracking controller, which was not applied during the HiL simulations.

It can be seen that the ground vehicle trajectory from the real-world experiment does not fully coincide with the HiL simulation results, which can be attributed to the aforementioned offset at the start of the trajectory, but also to dynamic effects that are neglected in the simulation model.

The maximum and mean execution time of the MPC task were 3.5 ms and 2.8 ms, respectively, which is well below the required sample time T_{MPC} of the MPC, allowing real-time execution on the given hardware.

The choice of parameters obtained from the simulations still yields feasible results in the real-world experiment. Although the tracking error observed in the real-world experiment is generally larger than in the simulation, it would allow safe landing of the UAV on the platform.

6. CONCLUSION

In this paper, a linear model-predictive trajectory tracking controller for a UGV in a heterogeneous rendezvous was presented. Based on a successively linearized kinematic bicycle model of the ground vehicle and a simple prediction model for the UAV assuming constant acceleration and yaw rate, a real-time capable MPC was proposed and compared against a Stanley based trajectory tracking controller. A constraint on the yaw rate of the ground vehicle was introduced in order to limit lateral acceleration. Thereby, sideslip is prevented and the consistency of the kinematic bicycle model is preserved. Simulative and experimental results were provided, demonstrating the feasibility of the proposed controller on a model-scale vehicle by means of a realistic reference trajectory. Despite the use of simple prediction models for both vehicles, the proposed controller was demonstrated to show sufficiently

Table 4. RMS and maximum absolute control error in real-world experiment with MPC

	ΔX(m)	ΔY(m)	$\Delta V(\frac{\text{m}}{\text{s}})$	$\Delta\Psi$(deg)
RMS	0.290	0.133	0.315	2.498
|max|	0.471	0.271	1.027	5.327

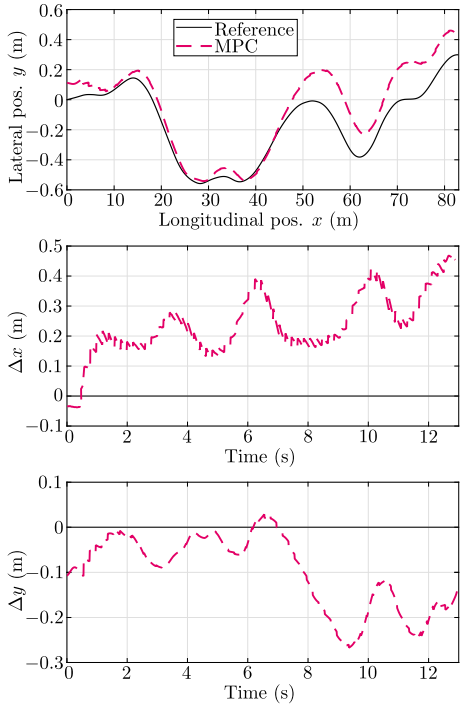

Fig. 6. Experimental results for the model predictive trajectory tracking controller

precise trajectory tracking for the UGV, as the longitudinal and lateral deviation remained below 0.5 m during the simulations and experiment. As the presented results are based on a single representative UAV trajectory, the general validity of the proposed approach should be examined further on the basis of a larger set of UAV trajectories.

Future research will aim at extending the proposed controller towards a cooperative control strategy and at investigating the impact of higher fidelity prediction models. By introducing higher fidelity vehicle models, significant improvements in tracking performance can be expected. However, this would come at the cost of higher computational complexity which must be considered regarding the real-time requirement of the application. A possible solution for enabling computationally more expensive control systems for solving the rendezvous problem would be to outsource the computations to a stationary unit, which introduces additional communication delays and sources of error. Furthermore, the robust absolute and relative positioning of the UAV and UGV is a crucial aspect in the heterogeneous rendezvous that will be considered in future research since even small dead-times in the communication link induce large positioning errors. For that purpose, the application of vision based real-time localization by means of fiducial markers could be a promising approach.

REFERENCES

Buehler, M., Iagnemma, K., and Singh, S. (2007). *The 2005 DARPA Grand Challenge: The Great Robot Race*, volume 36. Springer.

Camacho, E. and Alba, C. (2013). *Model Predictive Control*, 18–21. Advanced Textbooks in Control and Signal Processing. Springer London.

Falcone, P., Borrelli, F., Asgari, J., Tseng, H.E., and Hrovat, D. (2006). A Real-Time Model Predictive Control Approach for Autonomous Active Steering. *Nonlinear Model Predictive Control for Fast Systems, Grenoble, France*.

Ferreau, H., Kirches, C., Potschka, A., Bock, H., and Diehl, M. (2014). qpOASES: A Parametric Active-Set Algorithm for Quadratic Programming. *Mathematical Programming Computation*, 6(4), 327–363.

Hoffmann, G.M., Tomlin, C.J., Montemerlo, M., and Thrun, S. (2007). Autonomous Automobile Trajectory Tracking for Off-Road Driving: Controller Design, Experimental Validation and Racing. In *2007 American Control Conference*, 2296–2301. IEEE.

Kong, J., Pfeiffer, M., Schildbach, G., and Borrelli, F. (2015). Kinematic and Dynamic Vehicle Models for Autonomous Driving Control Design. In *2015 IEEE Intelligent Vehicles Symposium (IV)*, 1094–1099. IEEE.

Muskardin, T., Balmer, G., Persson, L., Wlach, S., Laiacker, M., Ollero, A., and Kondak, K. (2017). A Novel Landing System to Increase Payload Capacity and Operational Availability of High Altitude Long Endurance UAVs. *Journal of Intelligent & Robotic Systems*, 88(2-4), 597–618.

Persson, L., Muskardin, T., and Wahlberg, B. (2017). Cooperative Rendezvous of Ground Vehicle and Aerial Vehicle Using Model Predictive Control. In *2017 IEEE 56th Annual Conference on Decision and Control (CDC)*, 2819–2824. IEEE.

Persson, L. and Wahlberg, B. (2018). Verification of cooperative maneuvers in flightgear using mpc and backwards reachable sets. In *2018 European Control Conference (ECC)*, 1411–1416. IEEE.

Polack, P., Altché, F., d'Andréa Novel, B., and de La Fortelle, A. (2017). The Kinematic Bicycle Model: A Consistent Model for Planning Feasible Trajectories for Autonomous Vehicles? In *2017 IEEE Intelligent Vehicles Symposium (IV)*, 812–818. IEEE.

Reiter, M., Alrifaee, B., and Abel, D. (2014). Model Scale Experimental Vehicle as Test Platform for Autonomous Driving Applications. In *FISITA 2014 World Automotive Congress*.

Reiter, M., Abel, D., Rofalski, S., and Moormann, D. (2016a). GNSS-, Communication- and Map-Based Control System for Initiation of a Heterogeneous Rendezvous Maneuver. *IFAC-PapersOnLine*, 49(3), 171–177.

Reiter, M., Wehr, M., and Abel, D. (2016b). Built-in HiL simulator: A Concept for Faster Prototyping of Navigation- and Communication-Based Control Systems. In *2016 IEEE International Conference on Advanced Intelligent Mechatronics (AIM)*, 1363–1369. IEEE.

Rohacs, D., Voskuijl, M., and Siepenkotter, N. (2014). Evaluation of Landing Characteristics Achieved by Simulations and Flight Tests on a Small-Scaled Model Related to Magnetically Levitated Advanced Take-Off and Landing Operations. In *ICAS 2014: Proceedings of the 29th Congress of the International Council of the Aeronautical Sciences, St. Petersburg, Russia, 7-12 September 2014*. Citeseer.

Snider, J.M. et al. (2009). Automatic Steering Methods for Autonomous Automobile Path Tracking. *Robotics Institute, Pittsburgh, PA, Tech. Rep. CMU-RITR-09-08*.